CHEMPHYSCHEM

DOI: 10.1002/cphc.200800540

The Solvent-Dependent Shift of the Amide I Band of a Fully Solvated Peptide as a Local Probe for the Solvent Composition in the Peptide/Solvent Interface

Dietmar Paschek,*[a, b] Matthias Pühse,[a] Arnold Perez-Goicochea,[a] S. Gnanakaran,[c] Angel E. García,[d] Roland Winter,[a] and Alfons Geiger[a]

We determine the shift and line shape of the amide I band of a model AK peptide from molecular dynamics (MD) simulations of the peptide dissolved in methanol/water mixtures with varying composition. The IR spectra are determined from a transition dipole coupling exciton model. A simplified empirical model Hamiltonian is employed, which takes into account both the effect of hydrogen bonding and the intramolecular vibrational coupling. We consider a single isolated AK peptide in a mostly helical conformation, while the solvent is represented by 2600 methanol or water molecules, simulated for a pressure of 1 bar and a temperature of 300 K. Over the course of the simulations, minor reversible conformational changes at the termini are observed, which are found to only slightly affect the calculated spectral properties. Over the entire composition range, which varies from pure water to the pure methanol solvent, a monotonous shift towards higher frequency of the IR amide I band of about 8 wavenumbers is observed. This shift towards higher frequency is comparable to the shift found in preliminary experimental data also presented here on the amide I′ band. The shift is found to be caused by two counter-compensating effects. An intramolecular red shift of about 1.2 wavenumbers occurs, due to stronger intramolecular hydrogen bonding in a methanol-rich environment. Dominating, however, is the intermolecular solvent-dependent shift towards higher frequency of about 10 wavenumbers, which is attributed to the less effective hydrogen-bond-donor capabilities of methanol compared to water. The importance of the solvent contribution to the IR shift, as well as the significantly different hydrogen formation capabilities of water and methanol, makes the amide I band sensitive to composition changes in the local environment close to the peptide/solvent interface. This allows, in principle, an experimental determination of the composition of the solvent in close proximity to the peptide surface. For the AK peptide case, we observe at low methanol concentrations a significantly enhanced methanol concentration at the peptide/solvent interface, supposedly promoted by the partially hydrophobic character of the AK peptide's solvent-accessible surface.

1. Introduction

Alanine-rich peptides have been shown to form stable helices in an aqueous environment.[1] Numerous IR spectroscopic studies have focused on the thermodynamics and kinetics of helix formation by probing the temperature-induced unfolding transition.[1–6] Recent advances in computer simulation methodology have provided the opportunity to study the nature and structural inhomogeneity of helix formation in great detail.[7–9] Simulation data have delivered insights by predicting the shift and line shape of the amide I band, while taking into account both the effect of hydrogen bonding and intramolecular vibrational coupling.[7,9] Moreover, the pressure dependence of the amide I band revealed the importance of the solvent contribution to the pressure-induced red shift. The observed solvent-induced shift is found to be about three to four times larger than the contribution due to conformational changes of the peptide[9,10] or the "elastic compression" of the helix. The solvent effect on the IR spectrum has also been observed in pressure studies of poly(*N*-isopropylacrylamide) in aqueous solution,[11] where intramolecular hydrogen bonds play no role.

Herein, we utilize this solvent contribution to the amide I band to study the interaction of the peptide with co-solvents. The effect of co-solvents on the stability of proteins has been attributed to the specific solvent-mediated attractive or repulsive interaction of the co-solvent with the protein, which leads to a specific excess concentration of the co-solvent in the vicinity of the protein.[12–15] Most of those studies are based on the measurement of excess thermodynamic quantities, which are analyzed in the framework of Kirkwood–Buff theory, by assuming concentration changes localized at the protein sur-

[a] *Dr. D. Paschek, M. Pühse, A. Perez-Goicochea, Prof. Dr. R. Winter, Prof. Dr. A. Geiger*
Physikalische Chemie, Fakultät Chemie, TU Dortmund
Otto-Hahn-Str. 6, 44227 Dortmund (Germany)
Fax: (+49) 231 755 3748
E-mail: dietmar.paschek@uni-dortmund.de

[b] *Dr. D. Paschek*
Lehrstuhl Thermodynamik, Fakultät Bio- und Chemieingenieurwesen
TU Dortmund, Emil-Figge-Str. 70, 44227 Dortmund (Germany)

[c] *Dr. S. Gnanakaran*
Los Alamos National Laboratory, T10-MS K710
Los Alamos, NM 87545 (USA)

[d] *Prof. Dr. A. E. García*
Department of Physics, Applied Physics, and Astronomy
Rensselaer Polytechnic Institute
110 Eighth Street, Troy, NY 12180-3590 (USA)

face.[15] Herein, we focus on the effect of the changing solvent composition on the shift of the amide I band of a 20 amino acid alpha-helical AK peptide with sequence Ac-AA-(AAKAA)$_3$AAY-NMe. In contrast to our previous studies,[7,9] we investigate solvation changes of the mostly homogeneously folded state of the peptide found at low temperatures. Given that the conformational state of the peptide is only little affected, we suggest that the solvent-dependent shift of the amide I band may be employed to determine the local composition of the solvent in the vicinity of the peptide. Based on computer simulations of a realistic model system and from theoretically predicted IR spectra, we show that the water excess concentration in the vicinity of the peptide in a methanol/water mixture can be recovered from the location of the IR band with a reasonable degree of accuracy. We would like to emphasize that complementary experimental techniques, such as circular dichroism (CD) spectroscopy, have to be employed to make sure that the experimentally observed IR shifts are dominated by the changing solvent and only affected to a minor degree by alterations of the conformational ensemble of the peptide itself.

2. Methods

2.1. Details of the Molecular Simulations

We performed molecular dynamics (MD) simulations of a single AK peptide molecule in methanol/water mixtures with the compositions indicated in Table 1. Each simulated system contained 2600 solvent molecules in a cubic box with periodic boundary conditions. Water was represented by the three-center TIP3P model,[16] whereas methanol was described using the TraPPE united-atom force field.[17,18] For the AK peptide we employed the AMBER-94 force field[19] as modified by García and Sanbonmatsu.[20–22]

Table 1. Parameters characterizing the performed MD simulation runs.[a]

x_{MeOH}	Run length τ [ns]	Density $\langle\rho\rangle$ [kg m^{-3}]
0.0	40	992.39 ± 0.04
0.02	40	985.24 ± 0.03
0.05	40	974.91 ± 0.03
0.1	40	958.95 ± 0.03
0.2	40	930.37 ± 0.04
0.5	40	864.15 ± 0.03
1.0	40	787.61 ± 0.05

[a] All simulations were carried out at $T = 300$ K and $P = 1$ bar. Each simulation contained exactly 2600 solvent molecules plus one helical 20-residue AK peptide with sequence Ac-AA(AAKAA)$_3$AAY-NMe.

We performed MD simulations in the NPT ensemble using the Nosé–Hoover thermostat at $T = 300$ K[23,24] and the Rahman–Parrinello barostat[25,26] with coupling times $\tau_T = 1.5$ and $\tau_p = 2.5$ ps, assuming the isothermal compressibility to be $\chi_T = 4.5 \times 10^{-5}$ bar^{-1}. The electrostatic interactions were treated in the "full potential" approach by the smooth particle mesh Ewald summation[27] with a real-space cutoff of 0.9 nm and a mesh spacing of approximately 0.12 nm and fourth-order interpolation. The Ewald convergence factor α was set to 3.38 nm^{-1} (corresponding to a relative accuracy of the Ewald sum of 10^{-5}). A 2.0 fs time step was used for all simulations and the water constraints were solved using the SETTLE procedure,[28] while the SHAKE method was used to constrain the bond lengths[29] in methanol and the AK peptide. All bond lengths were kept fixed. All simulations reported here were carried out using the GROMACS 3.2 program.[30,31] The MOSCITO suite of programs[32] was employed to generate appropriate start configurations and topology files, and was used for the entire data analysis presented herein. The AK peptide was inserted into the mixture in its full helical state, and it was verified that it stayed in this state during the initial equilibration period. Production runs of length 40 ns were analyzed for each composition. Statistical errors in the analysis were computed with the method of Flyvbjerg and Petersen.[33] For all reported systems initial equilibration runs of length 1 ns were performed using the Berendsen weak coupling scheme for pressure and temperature control ($\tau_T = \tau_p = 0.5$ ps).[34]

2.2. Calculation of the IR Spectra

The sensitivity of the amide I band in alpha-helical proteins to hydration by water has been demonstrated experimentally.[35,36] In addition, the structural disorder of helical peptides has been investigated by the amount of inhomogeneous broadening in 1D and 2D IR spectroscopy.[6,37,38] Here, we used an empirical transition dipole coupling model[39–41] to simulate the trends associated with the amide I band that occur due to both solvation changes and structural relaxation of the AK peptide. It was assumed that the amide I manifold states can be separated from all other vibrational modes. The transition dipole coupling modified the nearly degenerate amide I modes and contributed to the off-diagonal terms of an exciton Hamiltonian matrix in the basis of these modes. These matrix elements can be approximated by the transition dipole–transition dipole term [Eq. (1)]:

$$\beta_{km} = \frac{\vec{\mu}_k \cdot \vec{\mu}_m - 3(\vec{\eta}_{km} \cdot \vec{\mu}_k)(\vec{\eta}_{km} \cdot \vec{\mu}_m)}{r_{km}^3} \quad (1)$$

where $\vec{\mu}_k$ is the effective transition dipole of the k-th amide I mode, $\vec{\eta}_{km}$ is the unit vector connecting the dipoles k and m, and r_{km} is the distance between the dipoles.[39] The empirical transition dipole moment has a magnitude of 0.305 D and is located 0.868 Å from the carbonyl carbon atom along the C=O bond, directed 20° from the C=O bond toward O→N.[42] The application of this empirical model must be cautioned, since the nearest-neighbor interaction may not be properly represented.[43]

The diagonal matrix elements of the Hamiltonian are sensitive to the amide I frequency shifts caused by coupling to other modes and to the solvent. The contribution to the amide I frequency fluctuations from hydrogen-bonding interactions between the peptide C=O bond and hydrogen-bond

donors was considered explicitly. Additional amide I frequency shifts dictated by fluctuations in geometry were neglected in our calculations. Frequency shifts due to hydrogen-bonding interactions were described in terms of geometrical considerations of the solvent molecules or internal atoms, which are suitably located to form a hydrogen bond to the C=O group.[44,45] We define a hydrogen bond as existing when the distance between the hydrogen atom of a donor and the oxygen atom of the peptide unit is less than the hydrogen-bond cutoff distance of 2.6 Å and makes favorable angles (C=O···H and O···H–X $>90^{o}$). When these constraints are satisfied, the diagonal shift in frequency $\delta\nu_H$ due to hydrogen bonding (in units of cm^{-1}) is given as [Eq. (2)]:

$$\delta\nu_H = D_H\left(r_{OH} - r_{OH}^C\right) \quad (2)$$

where $r_{OH}^C = 2.6$ Å and $D_H = 30\ cm^{-1}\,Å^{-1}$, and r_{OH} is the C=O···H–X distance given in Å.[7,9,44–47] When more than one hydrogen atom satisfied the above criteria, the shift was considered to be additive. For specific hydrogen bonding to carbonyl groups, the amide I shifts and the additive property are in quantitative agreement with ab initio calculations for structures near the equilibrium hydrogen-bond distances.[48–50] This empirical model works reasonably well for helical secondary structures. With this simple model we have been consistently able to capture the trends of the amide I band of helical peptides with respect to solvation, temperature, and pressure for the helix–coil transition.[7,9] Predictions based on this model have also been confirmed by measurements.[6,10] However, we are not sure how well this simple empirical model would translate into reproducing amide I bands of other secondary structures.

For each configuration, the Hamiltonian was constructed and diagonalized to obtain the excitonic frequencies and intensities. In the calculation of the amide I spectrum, a separation of timescales between homogeneous and inhomogeneous contributions is assumed. A typical[46] homogeneous dephasing time (T_2) of 0.8 ps was employed for all the investigated solvent compositions, thus leading to an intrinsic Lorentzian line shape with 13.2 cm^{-1} FWHM for each of the excitonic frequencies. The ensemble averaging of the frequency spectrum over all configurations obtained from the simulation naturally models the static inhomogeneous contribution to the spectrum, and the dephasing describes the motional narrowing in an ad hoc manner. The analysis was carried out for all seven simulations with different solvent compositions. The unperturbed frequency of an amide I oscillator was chosen to be $\nu_0 =$ 1659 cm^{-1}. The specific choice of ν_0 is not critical for our study because the interest is in the change of relative band shift and shape with respect to the changing solvation conditions.

3. Discussion

The simulated TIP3P/TraPPE methanol–water model solutions are found to satisfactorily reproduce the thermodynamic and structural properties that are experimentally observed at 300 K and atmospheric pressure. The calculated density variation follows nearly quantitatively the experimental data according to Coquelet et al.[51] (see Figure 1). The simulations do not show any phase separation tendency, as the calculated radial pair distribution functions (Figure 2) clearly suggest. Slight systematic deviations of the density are observed at lower concentrations, which lead to a somewhat larger slope of the density versus concentration curve, perhaps indicating a slightly larger partial molar volume of methanol at low concentrations. This observation could hint at a slight overestimation of the tendency of methanol to associate, compared to the real mixture.

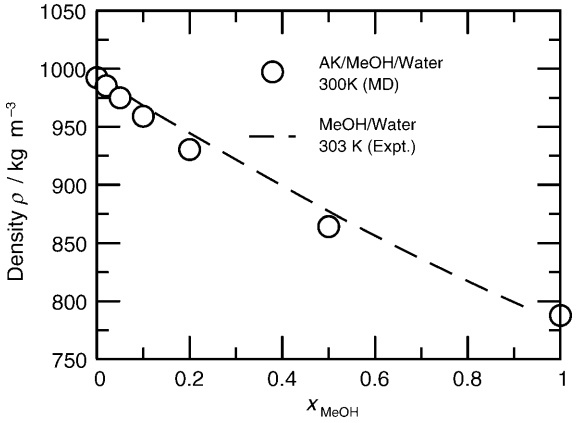

Figure 1. Experimental densities for binary methanol/water mixtures at $T = 303$ K[51] compared with data from our MD simulations.

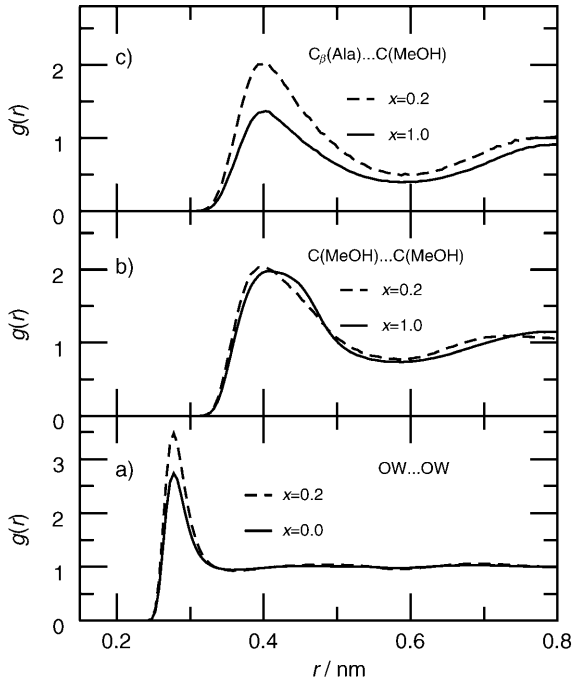

Figure 2. Comparison of radial distribution functions $g(r)$. a) Water–water oxygen correlations in pure water and at $x_{MeOH} = 0.2$. b) Methanol–methanol carbon correlations in pure methanol and at $x_{MeOH} = 0.2$. c) Correlations between methanol carbon and the C_β atom of the alanine residues of the AK peptide in pure methanol and at $x_{MeOH} = 0.2$.

The first peak features of the calculated radial pair distribution functions shown in Figure 2 are in good agreement with the data obtained from the neutron scattering experiments of Dougan et al.[53] and Dixit.[54] A first peak height of the water–water OW–OW pair distribution function increasing from 2.5 at $x_{MeOH}=0.0$ to about 3.5 at $x_{MeOH}=0.2$ matches almost exactly the data obtained from empirical potential structure refinement (EPSR) calculations reported in ref. [53], and determined from neutron scattering data. The observed water–water radial distribution functions, however, are a little less structured compared to what has been reported for methanol–water solutions in ref. [53], and for the structure of pure water.[55,56] This has been typically attributed to an underrepresented orientational (tetrahedral) order of neighboring water molecules, which is related to the TIP3P model's inability to reproduce water's anomalous thermodynamical features.[56,57] The almost concentration independence of height of the methanol–methanol carbon peak at a value of about 2 is an additional feature reported by Dougan et al.[53] However, the EPSR analysis[53] suggests a slightly decreasing first peak for the mixture, whereas in our simulation the peak height is almost unchanged. Nevertheless, we conclude the simulated mixtures behave, on a structural level, quite similarly to what has been characterized as a bipercolating mixture by Dougan et al.[53]

The snapshot of an $x_{MeOH}=0.2$ mixture shown in Figure 3 illustrates the 3D structural nature of the mixture beyond simple pair correlations. An analysis based on cluster-size distributions of hydrophobic methanol–methanol contacts in the water-rich region (not shown) indicates that for small cluster sizes, the distribution of cluster sizes approaches $P(s)\approx s^{-\tau}$ with an exponent of $\tau=2.18$, where s represents the number of molecules forming a cluster. The same value is observed for the case of random bond percolation on a 3D lattice close to the percolation transition, and supports the view of methanol and water as a bipercolating mixture, as proposed by Dougan et al.[53] The observation of percolation is a feature apparently not untypical for aqueous solutions and was first observed for the water network in THF/water mixtures by Oleinikova et al.,[58] and was also found later for the hydrophobic clustering of tertiary butanol (TBA) in TBA/water mixtures.[59] Quite interestingly, the broad cluster-size distribution also has implications for the structure of the solvent at the peptide/solvent interface. As the picture of the solvation shell of the AK peptide in Figure 3 suggests, the nanoheterogeneous nature is also reflected on the peptide surface and reveals a patchy structure of methanol and water clusters. One may envision a subtle interplay between the size and distribution of solvent composition fluctuations at protein surfaces and the possible conformational response of the protein, which seems worth exploring further in the future.[60]

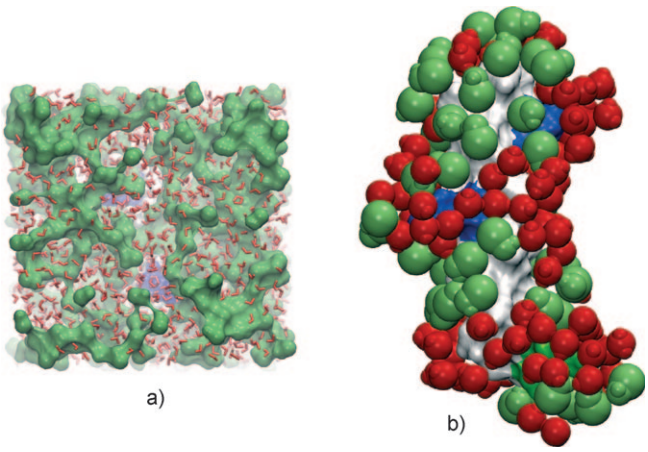

Figure 3. Pictorial representation[52] of snapshots taken from the simulation with $x_{MeOH}=0.2$. Left: Interdigitating networks of methanol and water in the bulk phase (methanol: green; water: red). Right: the peptide's solvent-accessible surface, as well as water and methanol molecules in the solvation layer.

Figure 2c shows the pair correlation functions between methanol carbon atoms and the methyl side chains of the alanine residues. The increase of the first peak at a concentration $x_{MeOH}=0.2$ compared to the pure methanol solutions indicates an increasing aggregation of methanol at low concentration, supposedly due to the partial hydrophobic character of the folded alanine helix. To elucidate the effect of partial aggregation, we inspected the water and methanol densities in close proximity to the peptide. We used a procedure of calculating the peptide–water proximal pair correlation functions $g_{prox}(R)$, similar to that used by Ashbaugh and Paulaitis,[61,62] as suggested earlier by others.[63,64] As reference sites we used heavy atoms of the peptide (C, N, O) and the center of mass of the solvent molecules. The normalization volume $s(r)dr$ is defined by volume elements with a shortest distance to any atom belonging to the set of peptide heavy atoms.

Figures 4a and 4b show the proximal radial distribution function between the peptide and methanol or water. The given $\rho_{prox}(R)$ values for water exhibit a typical two-peak feature, which has been reported to be characteristic of the hydration of polar and nonpolar atoms.[64,65] Note that the proportion between the two peaks is strongly concentration dependent and is markedly different for the pure liquid than for proteins reported hitherto,[64,65] with the nonpolar peak being more dominant for the AK peptide. This result suggests that the surfaces of larger-size proteins are, on average, significantly more polar than the surface of the AK peptide. For the case of methanol shown in Figure 4b, the two peaks are largely fused into one. From the densities of the individual components we calculate the local composition as a function of distance to the peptide according to Equation (3)

$$x_{MeOH}(R)=\frac{\rho_{MeOH}(R)}{\rho_{MeOH}(R)+\rho_{Water}(R)} \quad (3)$$

and shown in Figure 4c. The composition at the peak distance with $R\approx0.4$ nm indicates a more than twofold enhanced concentration of methanol at the solvation layer in the water-rich region. For large distances $R\rightarrow\infty$, $x_{MeOH}(R)$ converges to the composition of the bulk phase. The quantified "local" composition of the mixture at the interface (at $R\approx0.4$ nm) is given in Figure 4c and Table 2. The observed decrease of the $x_{MeOH}(R)$ for short distances shown in Figure 4c is an artifact based on the fact that we employed the center of mass of the molecules

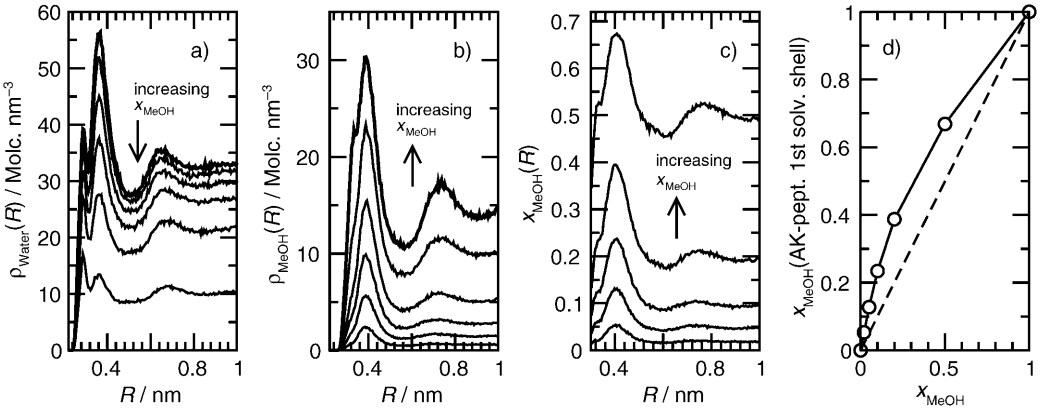

Figure 4. Solvent densities as obtained by proximal radial distribution functions of a) water and b) methanol as a function of the distance R normal to the peptide/solvent interface. c) Composition of the solvent as a function of the distance from the peptide/solvent interface. d) Composition of the solvent in the vicinity ($R \approx 0.4$ nm) of the peptide/solvent interface as a function of the bulk solvent composition.

Table 2. Parameters characterizing the location of the amide I band, as well as properties characterizing the solvation of the AK peptide in different methanol/water mixtures x_{MeOH}.[a]

x_{MeOH}	x_{MeOH}(local)	$\langle n_{CO}(OH)\rangle$	$\langle n_{CO}(OW)\rangle$	ν_{peak} [cm^{-1}]	$\langle \delta\nu_{intra}\rangle$ [cm^{-1}]	$\langle \delta\nu_{inter}\rangle$ [cm^{-1}]
0.0	0.0	–	1.108	1630.2	−12.93	−15.00
0.02	0.053	0.017	1.020	1631.0	−13.24	−14.07
0.05	0.127	0.040	0.933	1631.7	−13.46	−13.35
0.1	0.234	0.076	0.804	1632.7	−13.31	−12.50
0.2	0.387	0.113	0.630	1633.8	−13.58	−10.76
0.5	0.669	0.197	0.357	1635.7	−13.88	−8.45
1.0	1.0	0.294	–	1638.4	−14.19	−4.92

[a] Here, x_{MeOH}(local) characterizes the composition of the solvent in the vicinity of the peptide; $\langle n_{CO}(OW)\rangle$ and $\langle n_{CO}(OH)\rangle$ specify the carbonyl solvent oxygen coordination numbers for water (OW) and methanol (OH) as obtained from the corresponding radial distribution functions; ν_{peak} indicates the peak position of the calculated amide I band; and $\langle \delta\nu_{inter}\rangle$ and $\langle \delta\nu_{intra}\rangle$ represent the relative inter- and intramolecular shift contributions due to the effect of hydrogen bonding.

as reference, and that the water molecule has a smaller size compared to methanol.

The analysis of the composition of the solvation layer is complemented with a detailed description of the solvation of the carbonyl groups of the peptide by calculating the carbonyl oxygen coordination numbers (see Figure 5 and Table 2). The coordination number of about 1.1 in pure water is contrasted by an average coordination number of about 0.3 methanol molecules in the pure methanol liquid. Note that the obtained average coordination numbers are found to scale linearly with the "local" composition (compare values given in Table 2) of the solvent x^{l}_{MeOH} according to Equation (4)

$$n_{CO} = n^{*}_{CO}(MeOH) \times x^{l}_{MeOH} + n^{*}_{CO}(Water) \times \left[1 - x^{l}_{MeOH}\right] \quad (4)$$

The asterisk indicates the coordination number found in the pure solvent.

In previous studies it has been shown that side-chain shielding leads to a stabilization of solvated alpha-helical peptide.[7,20,66] For the AK peptide a residue-position-dependent alteration of the carbonyl hydration has been reported.[7] For low methanol concentrations a similar behavior is observed here, as the decreased coordination number of the carbonyl groups of lysine (at position i) and the neighboring alanine residue (at position $i-4$) indicate. Moreover, in line with the observations reported in ref. [7], the residues close to the C terminus also show strongly enhanced coordination numbers. As Figure 6 reveals, the methanol solvent exhibits the same coordination pattern as water, however, on a smaller scale. We would like to emphasize that this kind of alternating pattern is only observed in the water-rich region and is fully absent in the pure methanol solvent. It is apparently critically related to the hydration pattern of the backbone.[20] The large coordination number of the C-terminal residues is related to enhanced structural fluctu-

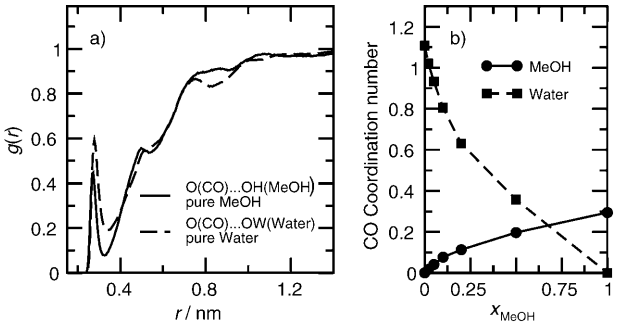

Figure 5. a) Oxygen–oxygen radial pair distribution function between the oxygen of the amide groups and the water oxygen in a pure water solvent, as well as the methanol oxygen in a pure methanol solvent. b) Water and methanol coordination numbers obtained from the first peak of the O(CO)–OH and O(CO)–OW radial pair distribution functions for all simulated mixtures.

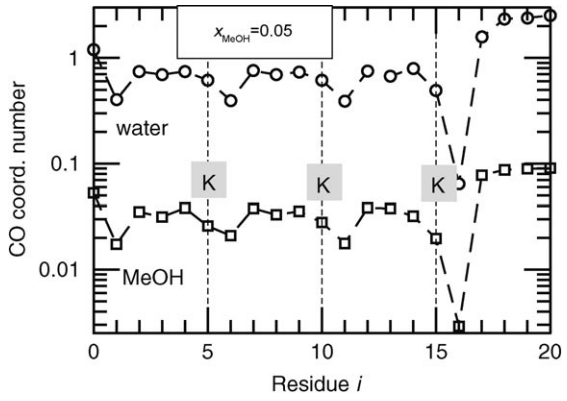

Figure 6. Water and methanol coordination numbers obtained from the first peak of the O(CO)–OH and O(CO)–OW radial pair distribution functions for $x_{MeOH} = 0.05$. The given coordination numbers are obtained for each residue individually.

ations observed at the termini and has been reported previously.[7]

Figure 7 describes the structural homogeneity of the simulated peptides in terms of its helical character. The helical content of the AK peptide is calculated according to the Lifson–

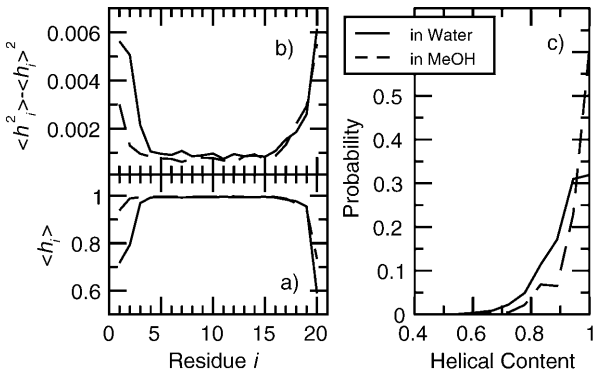

Figure 7. a) Probability of finding the *i*th residue in the alpha-helical state $\langle h_i \rangle$. b) Fluctuation of the helicity of the individual residues. c) Distribution of the helical content of the entire AK peptide.

Roig definition, which requires three consecutive residues to be helical.[67] Similarly to Refs. [7,8], the helical state of residue *i* is characterized when the (ϕ,ψ) angle lies in the alpha-helical region of the Ramachandran map $(\phi,\psi) = (-65 \pm 35, -37 \pm 30)$. The helicity $h_i = 1$ in the case $(\phi,\psi)_i$ are in the helical region, and $h_i = 0$ otherwise. The averages $\langle h_i \rangle$ characterize the fraction in a helical state, and the $\langle h_i^2 \rangle - \langle h_i \rangle^2$ indicate fluctuations of the helicity. Figures 7a and 7b indicate that the molecule in water and in methanol is predominantly helical, with small conformational alterations restricted to the terminal residues. The methanol solvent seems to stabilize the helical state for the terminal residues. Moreover, it not only suppresses the fluctuations at the termini, but also seems also to affect the conformational fluctuations of the middle residues around their alpha-helical equilibrium, as indicated by Figure 7b. The distribution of the helical content of the AK peptide (Figure 7c) is accordingly found to be shifted to slightly larger values. The average helical content increases from 0.92 (in water) to 0.96 (in methanol). Although the observed values reveal a strongly homogeneous helical structure of the peptide, they are compatible with data from REMD simulations of the AK peptide, for which a value of about 0.9 was reported for the lowest temperatures.[7] However, we cannot fully rule out a small bias towards the helical state due to the limited time window of our simulations. In addition, we would like to emphasize that the experimental data of Decatur[68] suggest that the simulated peptide is structurally too homogeneously helical.

Lastly, we would like to discuss the calculated spectral properties with changing solvent conditions predicted for the amide I band. Figure 8 shows the calculated amide I bands for

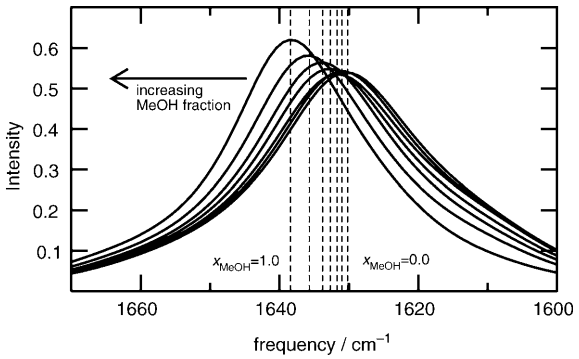

Figure 8. Calculated IR spectra for the AK peptide in methanol/water mixtures with the compositions $x_{MeOH} = 0.0, 0.02, 0.05, 0.1, 0.2, 0.5, 1.0$. The amide I band is found to shift monotonously from 1630.2 cm^{-1} (pure water) to 1638.4 cm^{-1} (pure methanol). The vertical lines indicate the peak positions.

all solvent compositions; the peak frequencies are given in Table 2. We observe a shift of the peak of the amide I band of about 8 wavenumbers to larger frequencies, which is quite similar to the shift associated with the helix–coil transition[6] and the 14 wavenumbers found in our preliminary experimental work discussed later (see Figure 12). In the present case, however, the observed simulated shift is apparently mostly due to the changing environment. In contrast to the behavior related the helix–coil transition, the peak intensity increases significantly and the line shape narrows slightly. Both features are apparently related to the increasing (helical) structural homogeneity observed for the peptide in a methanol environment.

To separate intramolecular from solvent contributions, we calculated the averages of the solvent shift contributions $\langle \delta\nu_H \rangle$ before employing excitonic mixing. The individual shift components are shown in Figure 9 and also given in Table 2. The different contributions are found to have a counter-compensating tendency. The intramolecular contribution leads to a red shift of about 1.2 wavenumbers, apparently due to the more homogeneous helical structure and more stable intramolecular hydrogen bonding. The solvent contribution, however, leads to a significant shift towards higher frequency of about 10 wavenumbers, about one order of magnitude larger than the intra-

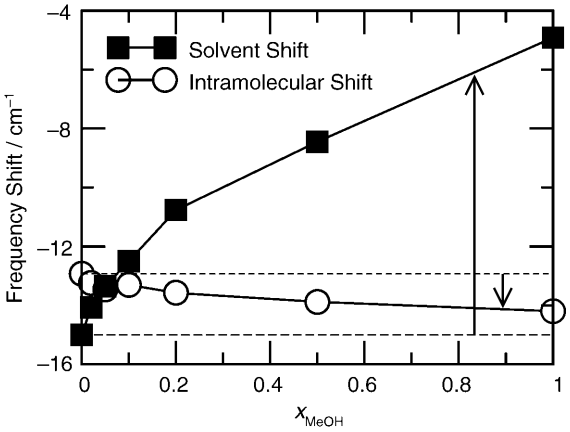

Figure 9. Inter- and intramolecular hydrogen-bond contributions to the shift of the amide I band as a function of the mixture composition. Interaction with the solvent leads to a shift towards higher frequency of about 10 wavenumbers, which is compensated by a red shift due to intramolecular hydrogen bonding of about 1.2 wavenumbers.

molecular contribution. We conclude that for a case where the conformational equilibrium of a peptide is mostly unaffected, the solvent can be the dominating contribution to the shift of the amide I band. This finding is qualitatively in line with the study of Starzyk et al.,[69] who observed a shift towards higher frequency of the amide I′ band of the helical peptide in trifluoroethanol/water mixtures, while CD spectroscopy indicated and enhanced helical order. Note that the frequency shift does not change linearly with the composition of the solvent.

A significantly increased slope of $\langle \delta\nu_H \rangle$ versus x_{MeOH} is observed in the water-rich region, which runs parallel with a nonlinearly changing coordination number of the carboxyl group (Figure 5), as well as the enhanced aggregation of methanol in the solvation layer of the AK peptide described in Figure 4d. Figure 10 suggests that the solvent contribution to the shift of the amide I band is linearly related to the average total coordination number of the carbonyl groups. This linear dependence and the relation between the coordination number n_{CO} and the local solvent composition x^l_{MeOH} given in Equation (4) suggest that the solvent contribution to the shift is linearly related to the local solvent composition [Eq. (5)]:

$$\langle \delta\nu_{inter} \rangle \propto n_{CO} \propto \left[n^*_{CO}(MeOH) - n^*_{CO}(Water) \right] \times x^l_{MeOH} + n^*_{CO}(Water) \quad (5)$$

The location of the peak position of the amide I as a function of the solvent composition shown in Figure 11 indicates that this feature is rather well preserved when including intramolecular contributions and even after excitonic mixing. The observed peak frequencies are a strongly nonlinear function of the mixture composition x_{MeOH}. However, they fall almost completely on the line connecting the peak positions of the pure liquids when the local compositions x^l_{MeOH} are used instead.

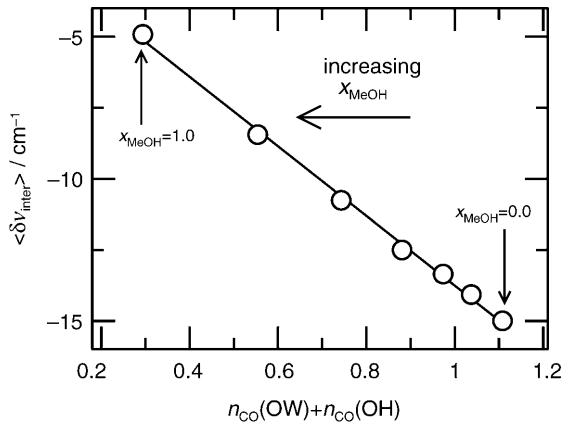

Figure 10. Correlation between the total coordination number (methanol plus water) and the calculated shift of the amide I band due to intermolecular hydrogen bonding.

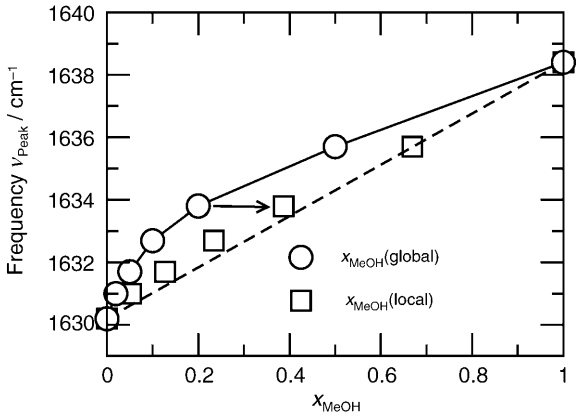

Figure 11. Location of the peak position of the amide I band as a function of the mixture composition. Here, x_{MeOH}(global) indicates the composition of the entire solvent, whereas x_{MeOH}(local) specifies the composition of the solvent in the vicinity of the peptide.

Finally, the experimental data shown in Figure 12 indicate that essential simulated features of the effect of changing solvent composition on the amide I band are also found in experimental IR spectra. On changing from a pure D_2O solvent to a pure $MeOD_4$ solvent, a shift towards higher frequency of about

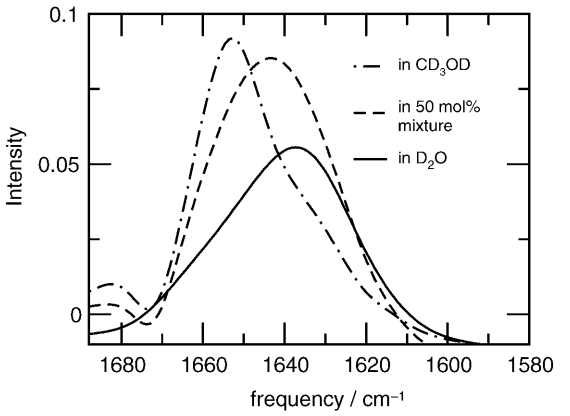

Figure 12. Experimental spectra of the amide I′ band for different methanol/water compositions obtained at 298 K.[60]

14 wavenumbers is observed. This shift is found in combination with an increasing intensity and an apparent narrowing of the peak. However, the peak in pure methanol appears to be less homogeneous than predicted by the MD simulations. The spectrum of the 50:50 mixture is found to be shifted halfway and exhibits an increased intensity compared to the spectrum obtained in pure D_2O, which is qualitatively in agreement with our predictions. Differences in the details between experimental and simulated spectra might be attributed to differences in the helical homogeneity observed in theory and experiment. To discuss these differences in detail would require knowledge of the full helix–coil transition of the simulated peptide with varying solvent composition. Hence, the contributions from differently folded (different helical propensity) ensembles could be analyzed in detail, as we have shown previously for the case of pure water by employing extensive replica exchange MD simulations.[7] Moreover, we can not rule out that the significant asymmetry observed for the spectra in MeOD is promoted by aggregation of the helices.

To summarize, although the shift of the peak is in the same range as that observed for the temperature-induced helix–coil transition, the peak features, such as peak height and width, might be used to distinguish it from the helix–coil transition. For the case of a very homogeneous, solvent-insensitive conformational distribution of the peptide, the peak shift is largely dominated by solvent contributions and is sensitive to the local composition of the solvent. A detailed analysis of the peak shift might be used to determine the local composition of the solvent in the vicinity of the peptide. We would like to emphasize that this procedure, used in combination with ^{13}C isotope labeling, seems to be suited to investigating the solvent composition close to partially solvated helices in larger proteins. For this case, the effect on the conformational equilibrium, largely suppressed by structural constraints, would also play a minor role.

4. Conclusions

We have determined the shift and line shape of the amide I band of a model AK peptide from MD simulations of the peptide dissolved in methanol/water mixtures with varying composition. The structural features of the simulated methanol/water mixtures are found to be in reasonable agreement with neutron scattering data, and show a patchy "bipercolating" clustering structure with a broad cluster-size distribution. For the AK peptide case, we observe at low methanol concentration a significantly enhanced (more than twofold) methanol concentration at the interface, supposedly due to the partially hydrophobic character of the AK peptide's solvent-accessible surface. The patchy structure of the liquid is also observed at the peptide surface. IR spectroscopic properties are determined from a transition dipole coupling exciton model. A simplified empirical model Hamiltonian is employed, which takes into account both the effect of hydrogen bonding and intramolecular vibrational coupling. We consider a single isolated AK peptide in the mostly folded state, while the solvent is represented by 2600 methanol or water molecules, simulated for a pressure of 1 bar and a temperature of 300 K. Over the course of the simulations minor reversible conformational changes at the termini are observed, which are found to not significantly affect the calculated properties. Over the entire composition range, from pure water to the pure methanol solvent, a monotonous nonlinear shift towards higher frequency of the IR amide I band of about 8 wavenumbers is observed. The shift of the peak is in the same range as that observed for the temperature-induced helix–coil transition; however, the peak features, such as increasing peak height and narrowing peak width, might be used to distinguish it from the helix–coil transition. The observed shift is found to be caused by two counter-compensating effects. An intramolecular red shift of about 1.2 wavenumbers occurs, due to stronger intramolecular hydrogen bonding in a methanol-rich environment. Dominating, however, is the intermolecular solvent-dependent shift towards higher frequency of about 10 wavenumbers, which is attributed to the less effective hydrogen-bond donor capabilities of methanol compared to water. The importance of the solvent contribution to the IR shift, as well as the significantly different hydrogen formation capabilities of water and methanol, makes the amide I band sensitive to composition changes in the local environment. Moreover, the calculated solvent shift is found to be linearly related to the (water/methanol) oxygen coordination number of the carboxyl groups and to the local methanol concentration. Hence, the composition of the solvent can be determined nearly quantitatively by the measuring the solvent-induced shift of the amide I band. A strongly nonlinear shift of the amide I band with respect to the composition is apparently a good indicator for significant methanol aggregation at the peptide/solvent interface. This feature could also allow the direct experimental determination of the composition of the solvent in close proximity to the peptide surface.

Acknowledgements

The AK peptide was kindly provided by Prof. Sean M. Decatur. A.G., R.W., and D.P. gratefully acknowledge financial support by the Deutsche Forschungsgemeinschaft (Forschergruppe 436). A.E.G. has been supported by the National Science Foundation (MCB-0543769). A.P.-G. gratefully acknowledges an IMPRS scholarship from the Max-Planck Society. We thank the ITMC at TU Dortmund for providing computer resources on LiDO.

Keywords: hydrogen bonds · IR spectroscopy · molecular dynamics · peptides · water chemistry

[1] S. Marqusee, V. H. Robbins, R. L. Baldwin, *Proc. Natl. Acad. Sci. USA* **1989**, *86*, 5286–5290.
[2] L. Vila, R. L. Williams, J. A. Grant, J. Woicik, H. A. Scheraga, *Proc. Natl. Acad. Sci. USA* **1992**, *89*, 7821–7825.
[3] G. Martinez, G. Millhauser, *J. Struct. Biol.* **1995**, *114*, 23–27.
[4] S. M. Decatur, J. Antonic, *J. Am. Chem. Soc.* **1999**, *121*, 11914–11915.
[5] R. A. G. D. Silva, J. Kubelka, P. Bour, S. M. Decatur, T. A. Keiderling, *Proc. Natl. Acad. Sci. USA* **2000**, *97*, 8318–8323.
[6] S. M. Decatur, *Acc. Chem. Res.* **2006**, *39*, 169–175.
[7] S. Gnanakaran, R. M. Hochstrasser, A. E. García, *Proc. Natl. Acad. Sci. USA* **2004**, *101*, 9229–9234.

[8] A. E. García, *Polymer* **2004**, *45*, 669–676.
[9] D. Paschek, S. Gnanakaran, A. E. García, *Proc. Natl. Acad. Sci. USA* **2005**, *102*, 6765–6770.
[10] S. M. Decatur, R. Winter, V. Smirnovas, *unpublished results*.
[11] F. Meersman, J. Wang, Y. Q. Wu, K. Heremans, *Macromolecules* **2005**, *38*, 8923–8928.
[12] T. Arakawa, S. N. Timasheff, *Biochemistry* **1982**, *21*, 6545–6552.
[13] S. N. Timasheff, *Annu. Rev. Biophys. Biomol. Struct.* **1993**, *22*, 67–97.
[14] S. N. Timasheff, *Adv. Protein Chem.* **1998**, *51*, 355–432.
[15] S. Shimizu, *Proc. Natl. Acad. Sci. USA* **2004**, *101*, 1195–1199.
[16] W. L. Jorgensen, J. Chandrasekhar, J. D. Madura, R. W. Impey, M. L. Klein, *J. Chem. Phys.* **1983**, *79*, 926–935.
[17] M. G. Martin, J. I. Siepmann, *J. Phys. Chem. B* **1998**, *102*, 2569–2577.
[18] B. Chen, J. J. Potoff, J. I. Siepmann, *J. Phys. Chem. B* **2001**, *105*, 3093–3104.
[19] W. D. Cornell, P. Cieplak, C. I. Bayly, I. R. Gouls, K. M. Merz, Jr., D. M. Ferguson, D. C. Spellmeyer, T. Fox, J. W. Caldwell, P. A. Kollman, *J. Am. Chem. Soc.* **1995**, *117*, 5179–5197.
[20] A. E. García, K. Y. Sanbonmatsu, *Proc. Natl. Acad. Sci. USA* **2002**, *99*, 2782–2787.
[21] S. Gnanakaran, A. E. García, *J. Phys. Chem. B* **2003**, *107*, 12555–12557.
[22] H. Nymeyer, A. E. García, *Proc. Natl. Acad. Sci. USA* **2003**, *100*, 13934–13939.
[23] S. Nosé, *Mol. Phys.* **1984**, *52*, 255–268.
[24] W. G. Hoover, *Phys. Rev. A* **1985**, *31*, 1695–1697.
[25] M. Parrinello, A. Rahman, *J. Appl. Phys.* **1981**, *52*, 7182–7190.
[26] S. Nosé, M. L. Klein, *Mol. Phys.* **1983**, *50*, 1055–1076.
[27] U. Essmann, L. Perera, M. L. Berkowitz, T. A. Darden, H. Lee, L. G. Pedersen, *J. Chem. Phys.* **1995**, *103*, 8577–8593.
[28] S. Miyamoto, P. A. Kollman, *J. Comput. Chem.* **1992**, *13*, 952–962.
[29] J. P. Ryckaert, G. Ciccotti, H. J. C. Berendsen, *J. Comput. Phys.* **1977**, *23*, 327–341.
[30] E. Lindahl, B. Hess, D. van der Spoel, *J. Mol. Model.* **2001**, *7*, 306–317.
[31] D. van der Spoel, E. Lindahl, B. Hess, A. R. van Buuren, E. Apol, P. J. Meulenhoff, D. P. Tieleman, A. L. T. M. Sijbers, K. A. Feenstra, R. van Drunen, H. J. C. Berendsen, *Gromacs User Manual version 3.2*, http://www.gromacs.org, **2004**.
[32] D. Paschek, MOSCITO 4 MD simulation package, http://ganter.chemie.tu-dortmund.de/MOSCITO, **2008**.
[33] H. Flyvbjerg, H. G. Petersen, *J. Chem. Phys.* **1989**, *91*, 461–466.
[34] H. J. C. Berendsen, J. P. M. Postma, W. F. van Gunsteren, A. DiNola, J. R. Haak, *J. Chem. Phys.* **1984**, *81*, 3684–3690.
[35] E. S. Manas, Z. Getahun, W. W. Wright, W. F. DeGrado, J. M. Vanderkooi, *J. Am. Chem. Soc.* **2000**, *122*, 9883–9890.
[36] S. T. R. Walsh, R. P. Cheng, W. W. Wright, D. O. V. Alonso, V. Daggett, J. M. Vanderkooi, W. F. DeGrado, *Protein Sci.* **2003**, *12*, 520–531.
[37] P. Mukherjee, I. Kass, I. Arkin, M. T. Zanni, *Proc. Natl. Acad. Sci. USA* **2006**, *103*, 3528–3533.
[38] P. Mukherjee, I. Kass, I. T. Arkin, M. T. Zanni, *J. Phys. Chem. B* **2006**, *110*, 24740–24749.
[39] S. Krimm, J. Bandekar, *Adv. Protein Chem.* **1986**, *38*, 181–364.
[40] H. Torii, M. Tasumi, *J. Chem. Phys.* **1992**, *96*, 3379–3387.
[41] A. Barth, C. Zscherp, *Q. Rev. Biophys.* **2002**, *35*, 369–430.
[42] J. F. Rabolt, W. H. Moore, S. Krimm, *Macromolecules* **1977**, *10*, 1065–1074.
[43] A. Moran, S. Mukamel, *Proc. Natl. Acad. Sci. USA* **2004**, *101*, 506–510.
[44] S. Gnanakaran, R. M. Hochstrasser, *J. Am. Chem. Soc.* **2001**, *123*, 12886–12898.
[45] S. Woutersen, P. Hamm, *J. Chem. Phys.* **2001**, *115*, 7737–7743.
[46] P. Hamm, M. H. Lim, R. M. Hochstrasser, *J. Phys. Chem. B* **1998**, *102*, 6123–6138.
[47] C. Scheurer, A. Piryatinski, S. Mukamel, *J. Am. Chem. Soc.* **2001**, *123*, 3114–3124.
[48] S. Ham, J. H. Kim, H. Lee, M. H. Cho, *J. Chem. Phys.* **2003**, *118*, 3491–3498.
[49] H. Torii, T. Tatsumi, M. Tasumi, *J. Raman Spectrosc.* **1998**, *29*, 537–546.
[50] H. Torii, T. Tatsumi, M. Tasumi, *J. Phys. Chem. B* **1998**, *102*, 309–314.
[51] J. Coquelet, A. Valtz, D. Richon, *J. Chem. Eng. Data* **2005**, *50*, 412–418.
[52] W. Humphrey, A. Dalke, K. Schulten, *J. Mol. Graphics* **1996**, *14*, 33–38.
[53] L. Dougan, S. P. Bates, R. Hargreaves, J. P. Fox, J. Crain, J. L. Finney, V. Réat, A. K. Soper, *J. Chem. Phys.* **2004**, *121*, 6456–6462.
[54] S. Dixit, J. Crain, W. C. K. Poon, J. L. Finney, A. K. Soper, *Nature* **2002**, *416*, 829–832.
[55] A. K. Soper, F. Bruni, M. A. Ricci, *J. Chem. Phys.* **1997**, *106*, 247–254.
[56] H. W. Horn, W. C. Sope, J. W. Pitera, J. D. Madura, T. J. Dick, G. L. Hura, T. Head-Gordon, *J. Chem. Phys.* **2004**, *120*, 9665–9678.
[57] D. Paschek, *J. Chem. Phys.* **2004**, *120*, 6674–6690.
[58] A. Oleinikova, I. Brovchenko, A. Geiger, B. Guillot, *J. Chem. Phys.* **2002**, *117*, 3296–3304.
[59] D. Paschek, A. Geiger, M. J. Hervé, D. Suter, *J. Chem. Phys.* **2006**, *124*, 154508.
[60] For the IR spectroscopic investigation of the amide I′ band of the AK peptide in dependence on different temperature and/or solvent conditions, we used an *N*-acetylated and *C*-amidated peptide (Ac-AA-$(AAKAA)_3$AAY-NH_2; kindly provided by S. M. Decatur). Experiments were carried out with deuterated solvents (D_2O and $MeOD_4$) due to the intense H-O-H bending vibration of water at about 1643 cm^{-1}, which interferes with the amide I region[70]. Peptide solutions (0.2%, w/v) were prepared by dissolving the corresponding amounts of peptide in D_2O or $MeOD_4$, and by mixing the solutions in the corresponding molar ratios (0, 50, or 100). FTIR measurements were performed using a Nicolet 5700 FTIR spectrometer. The applied MCT detector (HgCdTe) was cooled with liquid nitrogen. The sample (volume: 20 μL) was filled between CaF_2 windows, which were separated by a 50-μm-thick Mylar spacer. For temperature regulation, the cell was placed in a thermostated jacket with internal temperature measurement. An external water bath was used for temperature control (accuracy: ±0.2 °C). The sample chamber was purged constantly with dry air. Spectra were recorded from 4000 to 1100 cm^{-1}. To obtain accurate peak positions and to minimize spectral noise, 256 spectra were summed (spectral resolution: 2 cm^{-1}). Apodization was done with a Happ–Genzel function. Background subtraction (D_2O and $MeOD_4$) was performed with the temperature-corresponding solvent spectra with the respective factors, derived from the molar composition. Additionally, the carbonyl vibration of residual trifluoroacetic acid from peptide synthesis was carefully subtracted. The amide I′ band positions were determined with two significant digits with OMNIC 7.2 spectral processing software. For the pure solvents a temperature scan covering the range from 7 to 80 °C in 1 °C steps was performed. The temperature equilibration time before recording of spectra was 6 min. All other measurements were executed at 25 °C.
[61] H. S. Ashbaugh, M. E. Paulaitis, *J. Phys. Chem.* **1996**, *100*, 1900–1913.
[62] H. S. Ashbaugh, M. E. Paulaitis, *J. Am. Chem. Soc.* **2001**, *123*, 10721–10728.
[63] P. K. Mehrotra, D. L. Beveridge, *J. Am. Chem. Soc.* **1980**, *102*, 4287–4294.
[64] M. Levitt, R. Sharon, *Proc. Natl. Acad. Sci. USA* **1988**, *85*, 7557–7561.
[65] N. Smolin, R. Winter, *J. Phys. Chem. B* **2004**, *108*, 15928–15937.
[66] T. Ghosh, S. Garde, A. E. García, *Biophys. J.* **2003**, *85*, 3187–3193.
[67] S. Lifson, A. Roig, *J. Chem. Phys.* **1961**, *34*, 1963–1974.
[68] S. M. Decatur, *Biopolymers* **2000**, *54*, 180–185.
[69] A. Starzyk, W. Barber-Armstrong, M. Sridharan, S. M. Decatur, *Biochemistry* **2005**, *44*, 369–376.
[70] S. Y. Venyaminov, F. G. Prendergast, *Anal. Biochem.* **1997**, *248*, 234–245.

Received: August 15, 2008
Published online on November 26, 2008

